Predictive controllers for synchronous reluctance motor drive systems

Muhammad Syahril Mubarok[1], Nur Vidia Laksmi B.[2], Tian-Hua Liu[3]

[1]Department of Engineering, Faculty of Advanced Technology and Multidiscipline, Universitas Airlangga, Surabaya, Indonesia
[2]Department of Electrical Engineering, Universitas Negeri Surabaya, Surabaya, Indonesia
[3]Department of Electrical Engineering, National Taiwan University of Science and Technology, Taipei, Taiwan

Article Info	ABSTRACT
	This paper proposes the design and implementation of predictive controllers for synchronous reluctance motor drive systems to enhance their dynamic responses. The predictive speed and current controllers in this paper are designed in systematic procedures. The predictive speed controller is implemented by using Laguerre function procedure. The Laguerre function is used to simplify the algorithm and to minimize the execution time of the digital signal processor. For predictive current controller, a finite control set method improves the current tracking ability. The measured currents are used to predict the future phase-current based on the motor model. The optimal control inputs of both predictive controllers are determined by using a cost function minimization method. Experimental results show the proposed drive system provides a wide adjustable speed range, from 2 r/min to 1800 r/min. It has better performance than a proportional-integral (PI) controller including fast rise time, which is 0.9 second, small steady state error, which is 0.32 r/min, and small current ripples. A 32-bit floating-point digital signal processor, TMS-320-F-28335 DSP, is employed to implement the control algorithms. *This is an open access article under the CC BY-SA license.*

Corresponding Author:

Muhammad Syahril Mubarok
Department of Engineering, Faculty of Advanced Technology and Multidiscipline, Universitas Airlangga
Kuliah Bersama Building, Dr. Ir. H. Soekarno Street, Mulyorejo, Surabaya, East Java, 60115, Indonesia
Email: syahril.mubarok@ftmm.unair.ac.id

1. INTRODUCTION

Nowadays, the using of power electronics technology and control technology for AC motors has improved the performance of AC drive systems [1], [2]. AC motors are classified into three types: i) the induction motor, ii) the permanent magnet synchronous motor (PMSM), and iii) the synchronous reluctance motor (SynRM). The induction motor was commonly used in industry due to its low maintenance and simple structure. However, the PMSM has slighter size and higher performance than the induction motor does. The permanent magnet material used in PMSMs, however, is very expensive. To solve this problem, an emerging trend in the industry is to replace the PMSM with the SynRM, in which no permanent magnet material is required.

The SynRM has become more and more widespread due to its simple structure and no permanent magnet material is required [3]–[5]. The SynRM drive system is also very attracted compared to induction motor drive systems because its control strategies are more straightforward [6]. Additionally, the SynRM is free from rotor loss and slip, which provides higher efficiency and easier control than the induction motor.

The controller is an essential part for a motor drive system. There are various types of controllers that usually applied for SynRM drives. The simple way is using proportional-integral (PI) controller which the implementation is relatively straightforward. However, the tuning of PI parameter is more challenging for wide speed range [7]. Some advanced control of SynRM drive system have been examined by some researchers. Shyu and Lai [8] proposed multisegment sliding mode control for SynRM. The multisegment sliding mode controller was implemented for speed controller and the current loop used hysteresis controller. The method showed robust speed response but the ripple is huge. Lin *et al.* [9] proposed adaptive backstepping control for SynRM to improve speed tracking response. However, the result showed that the performance was good in middle to high speed. Senjyu *et al.* [10] proposed PI-based speed controller for SynRM with extended Kalman filter to achieve high efficiency control against parameter variation. Nevertheless, the method was too complicated when implemented in digital signal processor. Mahfoud *et al.* [11] proposed direct torque control strategy motor drives using model reference adaptive system. The method is used for sensorless speed control that is independent to the stator resistor. Accordingly, the dynamic response is quick.

Among the advanced control technique, the predictive controller has been successfully applied to industrial applications [12]. Generally, a model-based predictive controller (MBPC) requires a precise mathematical model of the motor [13]–[15]. Then, the future control signal trajectory should be predefined, and the output variable's future behaviors should also be optimized. A cost function minimization technique is added to calculate the optimal control input. As a result, the space-vector pulse width modulation (SVPWM) technique is not required here. The applications of the MPC include power converters [16]–[19] and motor drives [20]–[22]. Many previous papers have investigated the MBPC in either the current-loop control or the speed-loop control [23] but not including both of them in SynRM drive system.

In this paper, predictive controllers are proposed for SynRM drive in current loop and speed loop control system. A systematic design of MBPC improves the dynamics performances for SynRM. The control algorithm proposed in this paper is executed by using digital signal processor (DSP). Therefore, the hardware circuit is easy to design. Compared to previous research [1]-[23], the ideas in this paper, which include investigation of the speed-loop and current-loop predictive controllers for a SynRM drive systems, are original ideas.

2.   PREDICTIVE SPEED CONTROLLER DESIGN

In this paper, the speed loop of the SynRM drive system uses model predictive speed controller in which the Laguerre function procedure is employed. The predictive speed controller is designed based on the mechanical model of SynRM. The detailed model predictive speed controller design is explained in the following subsection.

2.1. Discrete model of SynRMs

The MBPC is a discrete-time controller. Therefore, the uncontrolled plant should also be presented in the discrete form as well. The discrete transfer function of the mechanical model of a SynRM can be represented as (1)-(3) [8].

$$G_p(z) \quad = \frac{\omega_{rm}(z)}{i_q(z)} = (1 - z^{-1})\mathbb{Z}\left(\frac{K_T/J_{m0}}{s+(B_{m0}/J_{m0})}\right) = \frac{h}{z-g} \tag{1}$$

According to (1):

$$h = \frac{K_T}{B_{m0}}\left[1 - e^{\frac{-B_{m0}}{J_{m0}}T_s}\right] \tag{2}$$

$$g = e^{\frac{-B_{m0}}{J_{m0}}T_s} \tag{3}$$

where J_{m0} is the inertia of the SynRM, B_{m0} is the friction coefficient of the SynRM, K_T is the constant torque, T_s is the sampling interval, and Z is the z-transformation. Then, by using the inverse z-transform of (1), it is not difficult to obtain as (4),

$$\omega_{rm}(n+1) = g\,\omega_{rm}(n) + hi_q(n) \tag{4}$$

where $\omega_{rm}(n + 1)$ is the predicted speed; $\omega_{rm}(n)$ is the measured speed; and $i_q(n)$ is the q-axis current.

2.2. Augmented model of SynRMs

According to (4) and taking into account the different operations on both sides [24], one can derive.

$$\Delta\omega_{rm}(n+1) = g\Delta\omega_{rm}(n) + h\Delta i_q(n) \tag{5}$$

Where $\Delta\omega_m(n+1)$ is the difference of predicted speed; $\Delta\omega_m(n)$ is the difference of present speed; and $\Delta i_q(n)$ is the difference of q-axis current. From (5) is expressed as (6).

$$\omega_{rm}(n+1) = g\Delta\omega_{rm}(n) + h\Delta i_q(n) + \omega_{rm}(n) \tag{6}$$

By subtracting $\omega_{rm}^*(n)$ of (6) on both sides, is defined as (7),

$$e_{\omega_{rm}}(n+1) = g\Delta\omega_{rm}(n) + h\Delta i_q(n) + e_{\omega_{rm}}(n) \tag{7}$$

where $e_{\omega_m}(n+1)$ and $e_{\omega_m}(n)$ are the speed errors, and $e_{\omega_m}(n)$ is expressed as (8).

$$e_{\omega_{rm}}(n) = \omega_{rm}(n) - \omega_{rm}^*(n) \tag{8}$$

Then the new state variable vector is selected as (9) [24].

$$X(n) = [\Delta\omega_{rm}(n) \quad \Delta\omega_{rm}(n-1) \quad \Delta i_q(n-1) \quad e_{\omega_{rm}}(n)]^T \tag{9}$$

By combining (5) and (7), yields.

$$\begin{bmatrix} \Delta\omega_{rm}(n+1) \\ e_{\omega_{rm}}(n+1) \end{bmatrix} = \begin{bmatrix} g & 0 \\ g & 1 \end{bmatrix} \begin{bmatrix} \Delta\omega_{rm}(n) \\ e_{\omega_{rm}}(n) \end{bmatrix} + \begin{bmatrix} h \\ h \end{bmatrix} \Delta i_q(k) \tag{10}$$

A new augmented state variable is defined as (11).

$$X(n+1) = \begin{bmatrix} \Delta\omega_m(n+1) \\ e_{\omega_{rm}}(n+1) \end{bmatrix} \tag{11}$$

And a new matrix and vector are expressed as (12) and (13).

$$A = \begin{bmatrix} g & 0 \\ g & 1 \end{bmatrix} \tag{12}$$

$$B = \begin{bmatrix} h \\ h \end{bmatrix} \tag{13}$$

Substituting (11)-(13) into (10), one can define (14) [24].

$$X(n+1) = AX(n) + B\Delta i_q(n) \tag{14}$$

According to (14), the output is defined as (15) and (16).

$$y(n) = CX(n) + \omega_{rm}^*(n) = \omega_{rm}(n) \tag{15}$$

$$C = [0 \quad 1] \tag{16}$$

2.3. Using Laguerre function for predictive controllers

A long control horizon can cause high computational numbers of the control signal $\Delta i_q(n)$. In this paper, the control horizon is used to capture the future control trajectory. As a result, the Laguerre function is applied here. First, $\Delta i_q(n)$ is represented as (17) [24].

$$\Delta i_q(n+p|n) = L(p)\eta(m) \tag{17}$$

Where p is the predictive step, $\eta(n)$ is the coefficient of Laguerre, and $L(p)$ is the Laguerre function vector. The predicted state variable vector is obtained as (18) and (19) [24].

$$X(n+p|n) = A^p X(k) + \varphi(p)^T \eta(n) \tag{18}$$

$$\varphi(p)^T = \sum_{d=0}^{p-1} A^{p-d-1} BL(d) \tag{19}$$

Where $\varphi(p)^T$ is the transition matrix. Then by replacing (18) into (15), is defined as (20).

$$\omega_{rm}(n+p|n) = CA^p X(n) + C\varphi(p)^T \eta + \omega_{rm}^*(n+p) \tag{20}$$

Then, the optimal actuation can then be determined by minimizing the cost function. The cost function is expressed as (21) [24].

$$J = \sum_{p=1}^{N_p} X(n+p|n)^T Q X(n+p|n) + \sum_{p=0}^{N_p-1} \Delta i_q(n+p)^T \frac{M_L}{L(p)^2} \Delta i_q(n+p) \tag{21}$$

Where N_p is the prediction horizon, M_L is constant and $Q = C^T C$ is the weighting matrix. Taking the partial derivative of (21), we can obtain the minimum cost function is defined as (22).

$$\frac{\partial J}{\partial \Delta i_q(n)} = \frac{1}{L(0)^2} 2\Delta i_q(n) \left(\sum_{p=1}^{N_p} \varphi(p) Q \varphi(p)^T + M_L \right) + \frac{1}{L(0)} 2X(n) \left(\sum_{p=1}^{N_p} \varphi(p) Q A^p \right) \tag{22}$$

The new variables in (22) can be defined as (23) and (24).

$$\Pi = \sum_{p=1}^{N_p} \varphi(p) Q \varphi(p)^T + M_L \tag{23}$$

$$\Lambda = \sum_{p=1}^{N_p} \varphi(p) Q A^p \tag{24}$$

From (22), we can set $\frac{\partial J}{\partial \Delta i_q(n)}$ to be 0, the optimal cost function is defined as (25).

$$\frac{\Delta i_q(n)}{L(0)} = -\Pi^{-1}\Lambda X(n) = \eta(n) \tag{25}$$

Finally, by substituting (25) into (17), the optimal solution of control input is derived as (26) and (27).

$$\Delta i_q(n) = -L(0)\Pi^{-1}\Lambda X(n) = -R_{mpc}X(n) \tag{26}$$

$$R_{mpc} = L(0)\Pi^{-1}\Lambda \tag{27}$$

Where R_{mpc} is the state feedback control gain.

In the real world, the SynRM control system should provide reasonable physical constraints on the state variables $\Delta i_q(n)$ and $i_q(n)$ to prevent saturation or damage to the hardware. The analytical solutions are required to identify the active constraints, which determine the control input $\Delta i_q(n)$ and $i_q(n)$. As result, the mathematical modifications are needed when the constraints are imposed in the system. The constraints of $\Delta i_q(n)$ and $i_q(n)$ are expressed as (28) [24].

$$\begin{bmatrix} \Delta i_q^{min} \\ i_q^{min} \end{bmatrix} \leq \begin{bmatrix} \Delta i_q(n) \\ i_q(n) \end{bmatrix} \leq \begin{bmatrix} \Delta i_q^{max} \\ i_q^{max} \end{bmatrix} \tag{28}$$

The MBPC for speed-loop is redesigned when the state variables in (28) satisfy the constraints using Hildreth's quadratic programming procedure [24]. In this paper, the constraint of the $\Delta i_q(n)$ is checked first. After that, the $i_q(n)$ is checked later to ensure that it is not exceeding the limit of the q-axis current. The MBPC for the speed-loop scheme is shown in Figure 1. The computations of the matrix and vector are simplified to simple numeric computations, which can be easily executed by a DSP.
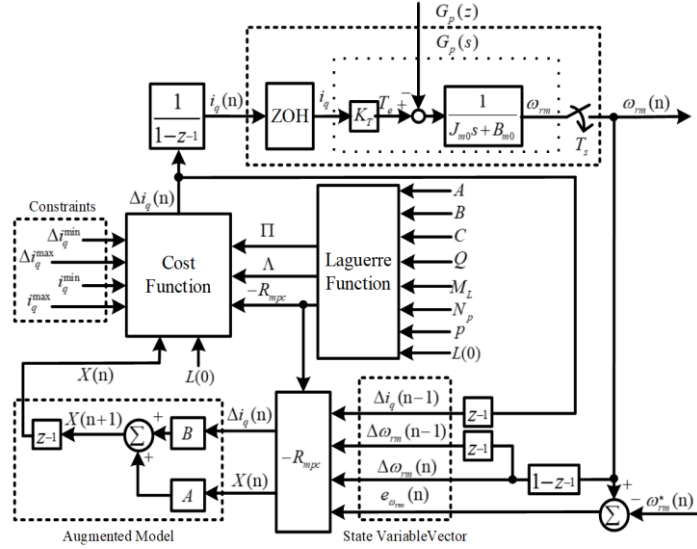
Figure 1. Predictive speed control scheme of the SynRM drive

3. MODEL-BASED PREDICTIVE CURRENT CONTROLLER DESIGN

In this paper, the focus is on a three phase, balanced, wye-connected SynRM. The three-phase stator voltage equation is expressed as (29) [25].

$$v_m = r_s i_m + L_q \frac{di_m}{dt} + e_m \tag{29}$$

Where m denotes the a-b-c-phase, v_m represents stator voltage generated by the inverter, r_s represents stator resistance, i_m represents the stator current, L_q represents the q-axis self-inductance, and e_m represents the extended back-EMF. The SynRM is driven by a three-phase voltage-source inverter (VSI) where the input power is dc-link voltage. The predicted stator current in the discrete-time form according to (29) is represented as (30) [25].

$$i_m^p(n+1) = \left(1 - \frac{r_s T_s}{L_q}\right) i_m(n) + \frac{T_s}{L_q}(v_m(n) - e_m(n)) \tag{30}$$

Where the superscript p denotes the predicted value; $i_m^p(n+1)$ is the predicted value of the stator current; $v_m(n)$ is the stator voltage; and $e_m(n)$ is the extended back-EMF. The time delay compensation is taken into account for the model-based predictive current controller design. Then according to (30), the predictive current can be expressed as (31) [26].

$$i_m^p(n+2) = \left(1 - \frac{r_s T_s}{L_q}\right) i_m^p(n+1) + \frac{T_s}{L_q}(v_m(n+1) - e_m(n+1)) \tag{31}$$

Where $i_m^p(n+2)$ is the predicted stator current; $v_m(n+1)$ is the predicted stator voltage; and $e_m(n+1)$ is the future extended back-EMF. The stator voltage is set to be constant because the sampling interval is very short. Therefore, the stator voltage at the $(n+1)$ and (n) sampling intervals are assumed to be the same. Moreover, in (31), the future extended back-EMF $e_m(n+1)$ cannot be measured. The extended back-EMF can be expressed as (32) [27].

$$e_m(n) \approx e_m(n-1) = v_m(n-1) - \left(\frac{r_s T_s + L_q}{T_s}\right) i_m(n) + \frac{L_q}{T_s} i_m(n-1) \tag{32}$$

According to (32), assumed $e_m(n+1) \approx e_m(n)$ due to the short sampling interval. Then (31) can be rewritten as (33) [27].

$$i_m^p(n+2) = \left(1 - \frac{r_s T_s}{L_q}\right) i_m^p(n+1) + \frac{T_s}{L_q}(v_m(n) - e_m(n-1)) \tag{33}$$

The minimum value of the cost function is obtained using a simple mechanism, it is expressed as (34) [25].

$$k = \left| (i_m^*(n) - i_m^p(n+2)) \right| \tag{34}$$

Where the symbol $*$ denotes the reference command. In (34), the cost function is composed of the predicted current error resulting from the deviation between the current command and the predicted current. The predictive current is obtained from the *d-q* axis currents, which is transformed into the *a-b-c* axis currents. Then according to (34), an optimal voltage vector can be defined as (35) [25].

$$k(n)|_{S_0,\dots,S_7} = min\{ k(n)|_{S_0}, \dots, k(n)|_{S_7} \} \tag{35}$$

The voltage vector obtained from (35) is implemented to manage the six switches of the inverter at the (n) sampling interval. Then, the model-based predictive current controller is responsible for determining the switching state of the inverter, as illustrated in Figure 2.
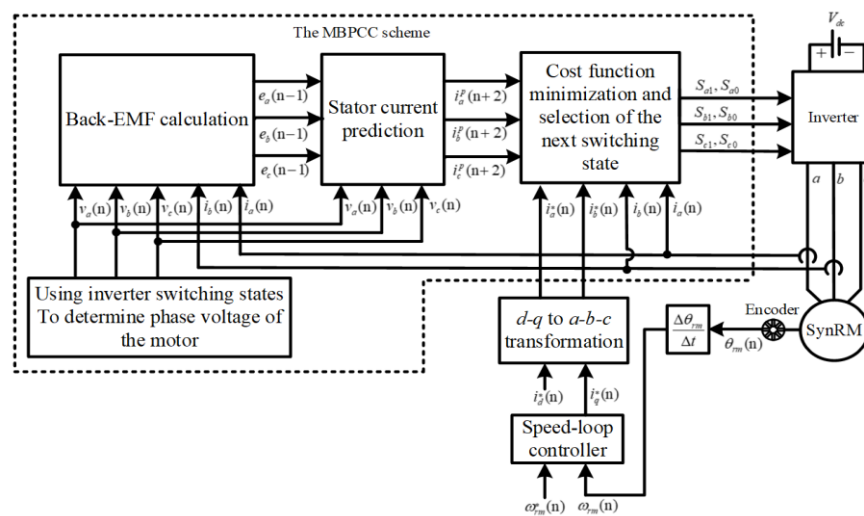
Figure 2. The MBPCC scheme for the SynRM drive

4.   IMPLEMENTATION

In the SynRM drives system is composed of two main components, the software and the hardware. The software is executed by a 32-bit floating-point TMS-320-F-28335 DSP, which is fabricated by Texas instruments. This DSP is employed to run the MBPC. The sampling interval of the speed-loop is 1 ms and the current-loop is 100 μs.

Figure 3(a) shows the block diagram of predictive controllers for SynRM drives is shown in Figure 3(a). The control algorithms in the software programs include the model-based predictive speed- and current-loop controllers, the *d-q* axis to *a-b-c* axis transformation, and a cost function minimization. The control algorithm starts with the speed command $\omega_{rm}^*(n)$ is an input command. Then, the MBPC executes the speed-loop to obtain the optimal value of the $i_q^*(n)$ while the $i_d^*(n)$ is set as a constant. This $i_q^*(n)$ is used for the current command in the current-loop. The *d-q* to *a-b-c* transformation frame is implemented because the current-loop control algorithm uses the *a-b-c* frame. By measuring the stator currents at the (n) sampling interval, we are able to determine the values of the stator currents at the $(n+2)$ sampling interval. Finally, a cost function minimization technique is used to determine the best candidate for the switching function. As the DSP only execute simple addition, subtraction, multiplication, and division. The computations of the matrix and vector are converted into simple calculations before the program is implemented.

Figure 3(b) illustrates the implementation of the SynRM drive system. The hardware consists of a SynRM, a three-phase VSI, some current and voltage sensing circuits, a reshaping circuit of encoder, and an interface circuit. The SynRM used in this paper is fabricated by Reliance Electric Company, type P56H5012. The motor parameters are as follows: L_q= 67.2 mH, L_d= 148 mH, R_s= 2.0 Ω, 4-pole, 3.4 A rated current, 220 V rated voltage, 560 W rated output power, and 1800 r/min rated speed.
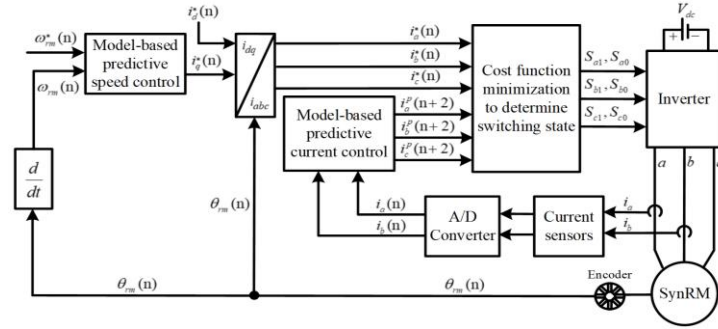
(a)
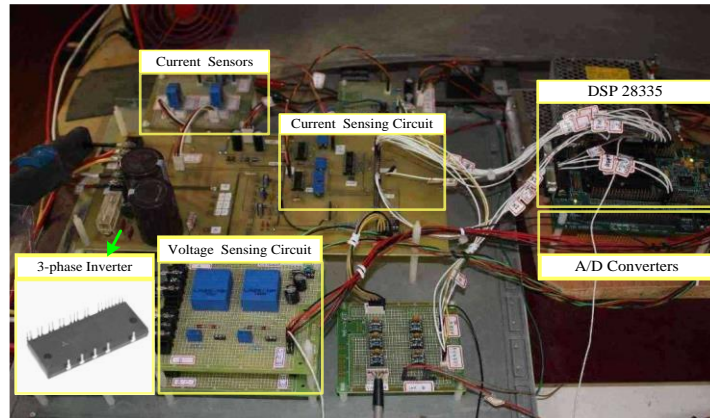
(b)

Figure 3. The implemented predictive controllers for SynRM drives: (a) block diagram and (b) hardware

5. EXPERIMENTAL RESULTS

There are several experimental results shown here to validate the proposed MBPC for SynRM drive systems. The detailed parameters are selected as follows: the d-axis current command $i_d^* = 0.5$, the initial value of Laguerre function $L(0) = 0.71$, the prediction horizon $N_p = 1$, and the current limitations including $\Delta i_q^{min} = -0.5A, \Delta i_q^{max} = 0.5A$, $i_q^{min} = -4A, i_q^{max} = 4A$. The prediction horizon is selected as 1 to simplify the required computation of the model-based predictive speed controller design.

Figures 4(a) and 4(b) show the predictive controller responses when the motor running from low speed to the rated speed. The different speed command with step input is given to evaluate the transient response. As can be observe from those figures, the proposed drive system has an adjustable speed range from 2 r/min to 1800 r/min with satisfactory performance.

(a)

(b)
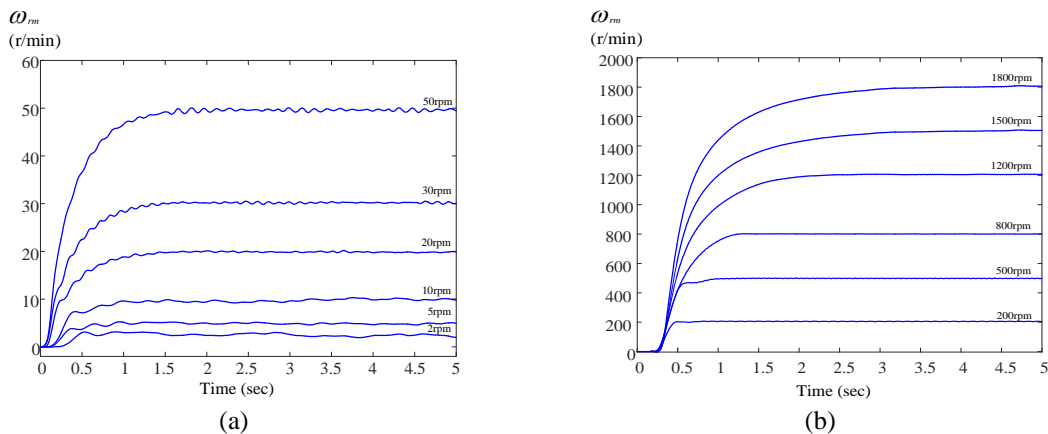
Figure 4. Transient responses at different speeds: (a) low speed and (b) high speed

Figure 5 show the results of the comparison of the proposed MBPC and the PI controller. These two controllers operate with and without load. Then, based on the pole assignment technique, the parameters of the PI current-loop and speed-loop controllers are determined. In this paper, the PI speed-loop controller is chosen as $K_p = 50$ and $K_i = 2$. On the other hand, the PI current-loop controller is chosen as $K_p = 50$ and $K_i = 5$. Figure 5 demonstrates the transient response with step command at 800 r/min. Compared to the PI controller, the MBPC has a faster transient response, including faster rise time and no overshoot before it converges to speed command. As well, it is important to note that the integral gain in the PI controller causes an overshoot in the speed response.

The rise time of the proposed MBPC is 0.9 second, while the PI controller is 1.6 second. The steady state error of the proposed MBPC is 0.32 r/min, while the PI controller is 6.6 r/min. The load disturbances responses at 500 r/min are shown in Figure 6 A 1 N.m external load are added to the drive system while it is running at steady-state. Once again, the proposed controller provides better performance than the PI controller. The MBPC has a small speed dip and a quick recovery time. Figures 7(a) and 7(b) show the measured speed responses to the sinusoidal speed commands using two different controllers. As can be observed, the predictive controller has better tracking responses than the PI controller for both positive half cycle and negative half cycle. As shown in Figure 8, different controllers are used to track current in the a-phase circuit. The proposed MBPCC can track the current command very well. Furthermore, the MBPCC has better current tracking responses and smaller current ripple than the PI controller.

Figures 9(a) and 9(b) show the measured current trajectory in the $\alpha - \beta$ frame when using the predictive controller and the PI controller. In Figure 9(a), the MBPC provides satisfactory current tracking with little current ripple. However, the PI controller has greater current ripple and has worse current tracking as shown in Figure 9(b). Figures 10(a) and 10(b) show the measured current errors in the $d - q$ frame. In Figure 10(a), the predictive controller has little current error. However, the PI controller has greater current error in the $d - q$ frame, which is shown in Figure 10(b). Actually, the current errors in the d-q frame that is shown in Figures 10(a) and 10(b) have DC offset. The DC offset is caused by the A/D converter does not convert the exact value at zero points.
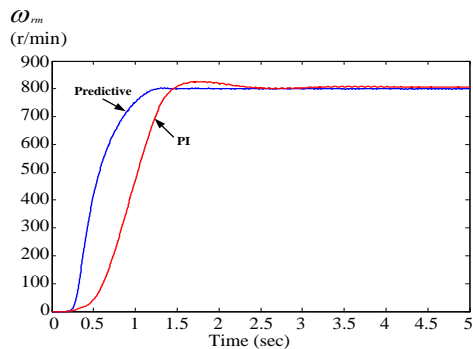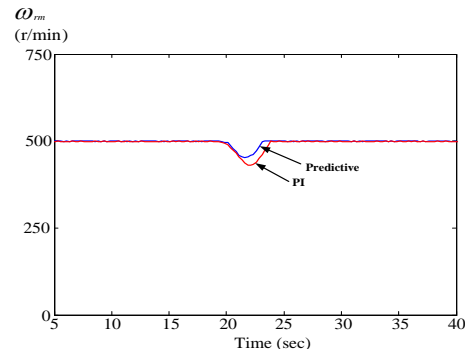

Figure 5. Comparison of transient responses

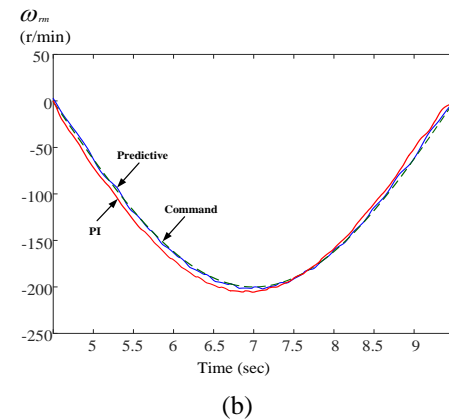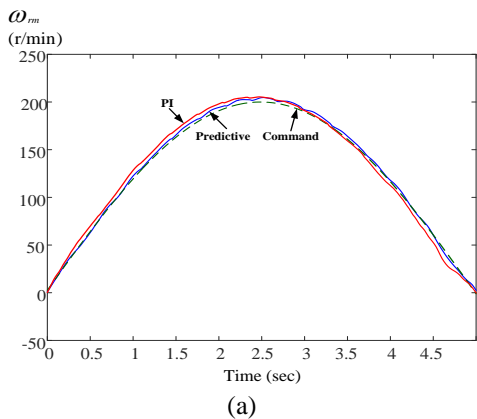Figure 6. Load disturbance responses at 1 N.m

(a)

(b)

Figure 7. Speed responses of a sinusoidal commands: (a) positive half cycle and (b) negative half cycle
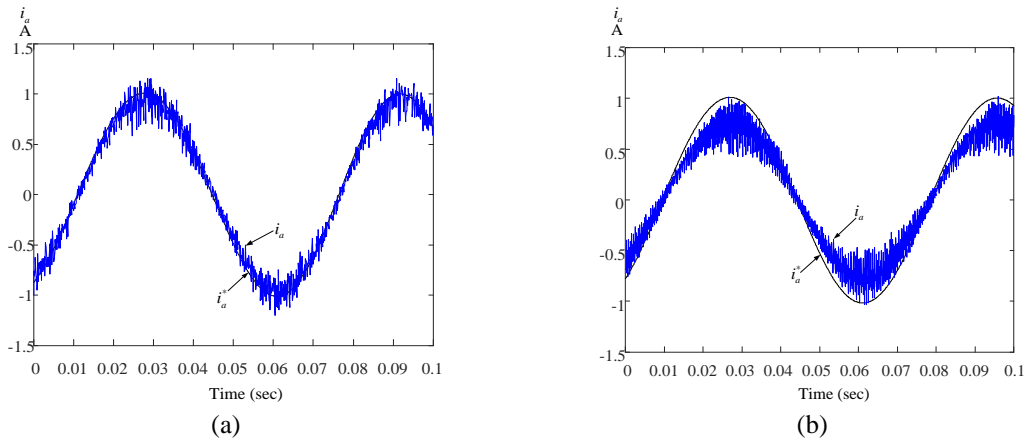
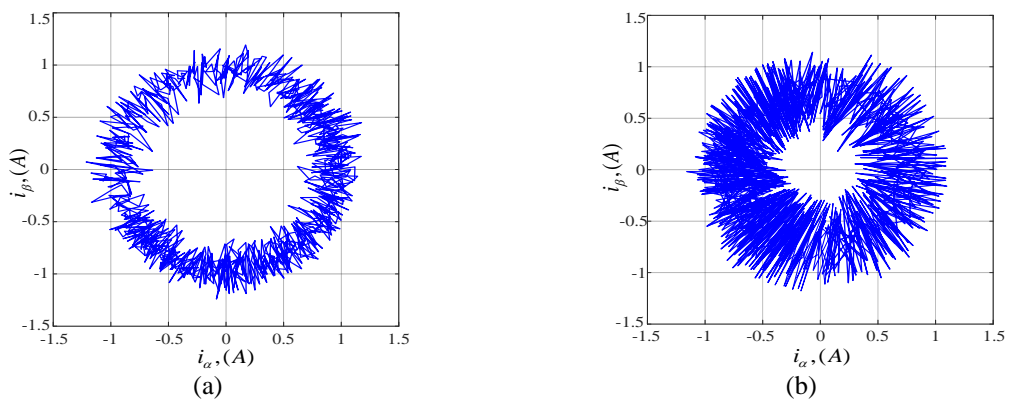Figure 8. Current tracking responses: (a) predictive and (b) PI

Figure 9. Current trajectories in the $\alpha - \beta$ frame: (a) predictive and (b) PI
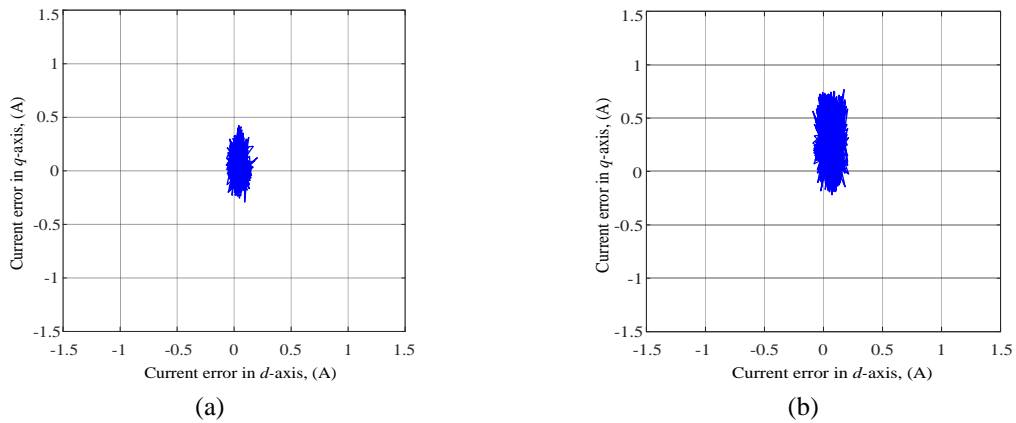

Figure 10. Current errors in the $d - q$ frame: (a) predictive and (b) PI

6. CONCLUSION

The design and implementation of a model-based predictive speed and current controller for a SynRM drive system is presented in this paper. Experimental results indicate that the proposed controllers are capable of achieving fast transient response and load disturbances response. In addition, the proposed controllers achieve wide adjustable speed from 2 r/min to 1800 r/min. In addition, the proposed drive system tracks the current command very well with small current errors. Although the analysis is complicated, the realization of the controllers is quite easy by using a DSP. The proposed predictive controllers can be

implemented in industrial application due to their satisfactory performance. However, the computational issue of the implemented predictive controllers for SynRM in this paper can be simplified in the future.

REFERENCES

[1]   D. Zhou, J. Zhao, and Y. Li, "Model-Predictive Control Scheme of Five-Leg AC–DC–AC Converter-Fed Induction Motor Drive," *IEEE Transactions on Industrial Electronics*, vol. 63, no. 7, pp. 4517–4526, Jul. 2016, doi: 10.1109/TIE.2016.2541618.

[2]   I. M. Alsofyani and K.-B. Lee, "A Unidirectional Voltage Vector Preselection Strategy for Optimizing Model Predictive Torque Control With Discrete Space Vector Modulation of IPMSM," *IEEE Transactions on Industrial Electronics*, vol. 69, no. 12, pp. 12305–12315, Dec. 2022, doi: 10.1109/TIE.2021.3134087.

[3]   S.-W. Park, T.-G. Woo, S.-C. Choi, H.-J. Lee, and Y.-D. Yoon, "Mitigating Rotor Movement During Estimation of Flux Saturation Model at Standstill for IPMSMs and SynRMs," *IEEE Transactions on Industrial Electronics*, vol. 70, no. 2, pp. 1171–1181, Feb. 2023, doi: 10.1109/TIE.2022.3159918.

[4]   J. Kolehmainen, "Synchronous Reluctance Motor With Form Blocked Rotor," *IEEE Transactions on Energy Conversion*, vol. 25, no. 2, pp. 450–456, Jun. 2010, doi: 10.1109/TEC.2009.2038579.

[5]   J.-B. Im, W. Kim, K. Kim, C.-S. Jin, J.-H. Choi, and J. Lee, "Inductance Calculation Method of Synchronous Reluctance Motor Including Iron Loss and Cross Magnetic Saturation," *IEEE Transactions on Magnetics*, vol. 45, no. 6, pp. 2803–2806, 2009, doi: 10.1109/TMAG.2009.2018663.

[6]   J. Riccio *et al.*, "Modulated Model-Predictive Integral Control Applied to a Synchronous Reluctance Motor Drive," *IEEE Journal of Emerging and Selected Topics in Power Electronics*, vol. 11, no. 3, pp. 3000–3010, Jun. 2023, doi: 10.1109/JESTPE.2023.3245077.

[7]   C.-C. Yu, *Autotuning of PID Controllers*. London: Springer London, 1999. doi: 10.1007/978-1-4471-3636-1.

[8]   K.-K. Shyu and C.-K. Lai, "Incremental motion control of synchronous reluctance motor via multisegment sliding mode control method," *IEEE Transactions on Control Systems Technology*, vol. 10, no. 2, pp. 169–176, Mar. 2002, doi: 10.1109/87.987062.

[9]   F.-J. Lin, M.-S. Huang, S.-G. Chen, C.-W. Hsu, and C.-H. Liang, "Adaptive Backstepping Control for Synchronous Reluctance Motor Based on Intelligent Current Angle Control," *IEEE Transactions on Power Electronics*, vol. 35, no. 7, pp. 7465–7479, Jul. 2020, doi: 10.1109/TPEL.2019.2954558.

[10] T. Senjyu, K. Kinjo, N. Urasaki, and K. Uezato, "High efficiency control of synchronous reluctance motors using extended kalman filter," *IEEE Transactions on Industrial Electronics*, vol. 50, no. 4, pp. 726–732, Aug. 2003, doi: 10.1109/TIE.2003.814998.

[11] M. El Mahfoud, B. Bossoufi, N. El Ouanjli, S. Mahfoud, M. Yessef, and M. Taoussi, "Speed Sensorless Direct Torque Control of Doubly Fed Induction Motor Using Model Reference Adaptive System," in *Digital Technologies and Applications*, Springer, 2021, pp. 1821–1830. doi: 10.1007/978-3-030-73882-2_165.

[12] J. Rodriguez and P. Cortes, *Predictive Control of Power Converters and Electrical Drives*. John Wiley & Sons, Ltd, 2012. doi: 10.1002/9781119941446.

[13] U. R. Muduli and R. Kumar Behera, "High Performance Finite Control Set Model Predictive DTC for Three-to-Five Phase Direct Matrix Converter Fed Induction Motor Drive," in *2021 22nd IEEE International Conference on Industrial Technology (ICIT)*, Mar. 2021, pp. 198–202. doi: 10.1109/ICIT46573.2021.9453475.

[14] O. Gulbudak and M. Gokdag, "FPGA-Based Model Predictive Control for Power Converters," in *2020 2nd Global Power, Energy and Communication Conference (GPECOM)*, Oct. 2020, pp. 30–35. doi: 10.1109/GPECOM49333.2020.9247873.

[15] O. Gulbudak and E. Santi, "FPGA-Based Model Predictive Controller for Direct Matrix Converter," *IEEE Transactions on Industrial Electronics*, vol. 63, no. 7, pp. 4560–4570, Jul. 2016, doi: 10.1109/TIE.2016.2546223.

[16] B. Long *et al.*, "Passivity-Based Partial Sequential Model Predictive Control of T-Type Grid-Connected Converters With Dynamic Damping Injection," *IEEE Transactions on Power Electronics*, vol. 38, no. 7, pp. 8262–8281, Jul. 2023, doi: 10.1109/TPEL.2023.3266588.

[17] A. Mora *et al.*, "Optimal Switching Sequence MPC for Four-Leg Two-Level Grid-Connected Converters," *IEEE Journal of Emerging and Selected Topics in Power Electronics*, 2023, doi: 10.1109/JESTPE.2023.3265502.

[18] Y. Li, S. Sahoo, T. Dragičević, Y. Zhang, and F. Blaabjerg, "Stability-Oriented Design of Model Predictive Control for DC/DC Boost Converter," *IEEE Transactions on Industrial Electronics*, vol. 71, no. 1, pp. 922–932, Jan. 2024, doi: 10.1109/TIE.2023.3247785.

[19] J. D. Barros, J. F. A. Silva, and E. G. A. Jesus, "Fast-Predictive Optimal Control of NPC Multilevel Converters," *IEEE Transactions on Industrial Electronics*, vol. 60, no. 2, pp. 619–627, Feb. 2013, doi: 10.1109/TIE.2012.2206352.

[20] S. H. Kim and K.-K. K. Kim, "Model Predictive Control for Energy-Efficient Yaw-Stabilizing Torque Vectoring in Electric Vehicles With Four In-Wheel Motors," *IEEE Access*, vol. 11, pp. 37665–37680, 2023, doi: 10.1109/ACCESS.2023.3266330.

[21] S. Bolognani, S. Bolognani, L. Peretti, and M. Zigliotto, "Design and Implementation of Model Predictive Control for Electrical Motor Drives," *IEEE Transactions on Industrial Electronics*, vol. 56, no. 6, pp. 1925–1936, Jun. 2009, doi: 10.1109/TIE.2008.2007547.

[22] P. G. Carlet, A. Favato, S. Bolognani, and F. Dorfler, "Data-Driven Continuous-Set Predictive Current Control for Synchronous Motor Drives," *IEEE Transactions on Power Electronics*, vol. 37, no. 6, pp. 6637–6646, Jun. 2022, doi: 10.1109/TPEL.2022.3142244.

[23] T.-H. Liu, H. S. Haslim, and S.-K. Tseng, "Predictive speed-loop controller design for a synchronous reluctance drive system," in *2016 International Symposium on Fundamentals of Electrical Engineering (ISFEE)*, Jun. 2016, pp. 1–6. doi: 10.1109/ISFEE.2016.7803196.

[24] L. Wang, *Model Predictive Control System Design and Implementation Using MATLAB®*. London: Springer London, 2009. doi: 10.1007/978-1-84882-331-0.

[25] C.-K. Lin, J. Yu, Y.-S. Lai, and H.-C. Yu, "Improved Model-Free Predictive Current Control for Synchronous Reluctance Motor Drives," *IEEE Transactions on Industrial Electronics*, vol. 63, no. 6, pp. 3942–3953, Jun. 2016, doi: 10.1109/TIE.2016.2527629.

[26] P. Cortes, J. Rodriguez, C. Silva, and A. Flores, "Delay Compensation in Model Predictive Current Control of a Three-Phase Inverter," *IEEE Transactions on Industrial Electronics*, vol. 59, no. 2, pp. 1323–1325, Feb. 2012, doi: 10.1109/TIE.2011.2157284.
[27] P. Cortes, J. Rodriguez, D. E. Quevedo, and C. Silva, "Predictive Current Control Strategy With Imposed Load Current Spectrum," *IEEE Transactions on Power Electronics*, vol. 23, no. 2, pp. 612–618, Mar. 2008, doi: 10.1109/TPEL.2007.915605.

BIOGRAPHIES OF AUTHORS

Muhammad Syahril Mubarok received his B.A.Sc. degree from the Electronic Engineering Polytechnic Institute of Surabaya, Indonesia, in 2015, and M.Sc. and Ph.D. degrees in electrical engineering from the National Taiwan University of Science and Technology, Taipei, Taiwan, in 2018 and 2023, respectively. His research interests include electric drive systems and model predictive control. Currently, he is a lecturer in the Department of Engineering, Universitas Airlangga, Surabaya, Indonesia. He can be contacted at email: syahril.mubarok@ftmm.unair.ac.id.

Nur Vidia Laksmi B. received her B.A.Sc. degree from the Electronic Engineering Polytechnic Institute of Surabaya, Indonesia, in 2015 and her M.Sc. degree from the Department of Electrical Engineering, National Taiwan University of Science and Technology (NTUST), Taiwan, in 2018. Currently, she is a lecturer in the Department of Electrical Engineering, Universitas Negeri Surabaya, Surabaya, Indonesia. Her research interests include power electronics, motor drives, and the application of control theories. She can be contacted at email: nurvidialaksmi@unesa.ac.id.

Tian-Hua Liu received his B.S., M.S., and Ph.D. degrees from the National Taiwan University of Science and Technology (NTUST), Taiwan. He is currently a Distinguished Professor at NTUST. His research interests include motor controls and power electronics. He can be contacted at email: liu@mail.ntust.edu.tw.